1990

Mathematical Model of a Lithium/Polypyrrole Cell

Taewhan Yeu
Texas A & M University - College Station

Ralph E. White
University of South Carolina - Columbia, white@cec.sc.edu

Publication Info

Journal of the Electrochemical Society, 1990, pages 1327-1336.

DOI: 10.1149/1.2086668
http://dx.doi.org/10.1149/1.2086668

JOURNAL OF THE ELECTROCHEMICAL SOCIETY

ELECTROCHEMICAL SCIENCE AND TECHNOLOGY

MAY 1990

EST

Mathematical Model of a Lithium/Polypyrrole Cell

Taewhan Yeu* and Ralph E. White**

Department of Chemical Engineering, Texas A&M University, College Station, Texas 77843-3122

ABSTRACT

A mathematical model to simulate the charge/discharge behavior of a lithium/lithium perchlorate-propylene carbonate/polypyrrole ($Li/LiClO_4$-PC/PPy) secondary battery cell is presented. The model can be used to gain a better understanding of the behavior of this cell and to provide guidance toward the design of new secondary batteries which utilize an electronically conductive polymer such as polypyrrole (PPy) as the cathode. The model includes the capability of handling charge and discharge behavior and is used to study the effect of various design parameters on the performance of the cell.

In recent years, much research has been done on the lithium/polypyrrole (Li/PPy) secondary battery system (1-5). Combining PPy with lithium in a secondary battery provides an inexpensive and noncorrodible battery with a high cell potential and unusual design flexibility. Several authors (1-5) have investigated the charge/discharge behavior of a Li/PPy cell.

Münstedt *et al.* (1) built and tested thin $Li/LiClO_4$-PC/PPy cells which showed excellent cyclability and stability without significant loss of capacity. PPy was found to be far superior to polyacetylene as an electrode material. Osaka *et al.* (2-3) obtained a high charge-discharge efficiency for a $Li/LiClO_4$-PC/PPy cell. Using potential step chronoamperometry together with ac impedance measurements, they observed a strong relationship between doping charges and the apparent diffusion coefficients for species in the PPy electrode. Their data suggested that the morphology of thin PPy films is an important factor in determining the electrochemical kinetics of the dopants in PPy films. Trinidad *et al.* (4) observed that the coulombic efficiency for these batteries is better than 90%. They suggested that it is necessary to increase the capacity of the cell and decrease the losses in cycling for full utilization of PPy as a cathode in a rechargeable lithium cell. Panero *et al.* (5) observed a high charge rate, a high coulombic efficiency, and a good cyclability of a PPy film electrode. Naoi *et al.* (6-7) reported the superiority of the charging-discharging performance of lithium batteries employing modified PPy with nitril rubber. The PPy film formed with the aid of nitril rubber showed a highly enhanced anion doping-undoping process because it has a rough, porous structure in the direction perpendicular to the current collector substrate.

Although the Li/PPy system has already attracted considerable attention in battery technology as discussed above, a secondary battery system based on the PPy is still in the experimental stage and the charge transport process within the solid PPy is not fully understood. To gain a better understanding of the dynamic behavior and to provide guidance toward better designs of new secondary batteries utilizing electrochemically conductive PPy, a one-dimensional mathematical model is presented here for the Li/PPy system. The model is an extension of previous work (8), which consists of a model to simulate potentiostatic cyclic voltammograms for a PPy film on a rotating disk electrode. A whole prismatic cell is considered here, consisting of a PPy positive electrode which has been electrochemically synthesized on a platinum current collector, a reservoir containing the electrolyte, a separator consisting of a porous inert material, and a lithium metal negative electrode.

The model is used to predict the dynamic behavior of the cell during charge and discharge at constant applied current density. The spatial and time dependence of concentration, overpotential, and electrode capacity profiles within the cell are presented. Also, the effects of various design parameters, such as the thickness of the PPy electrode, the reservoir, and the separator, are discussed.

Description of System

Figure 1 shows schematically the $Li/LiClO_4$-PC/PPy secondary battery system used in this study. The cell contains a platinum current collector which is electrochemically

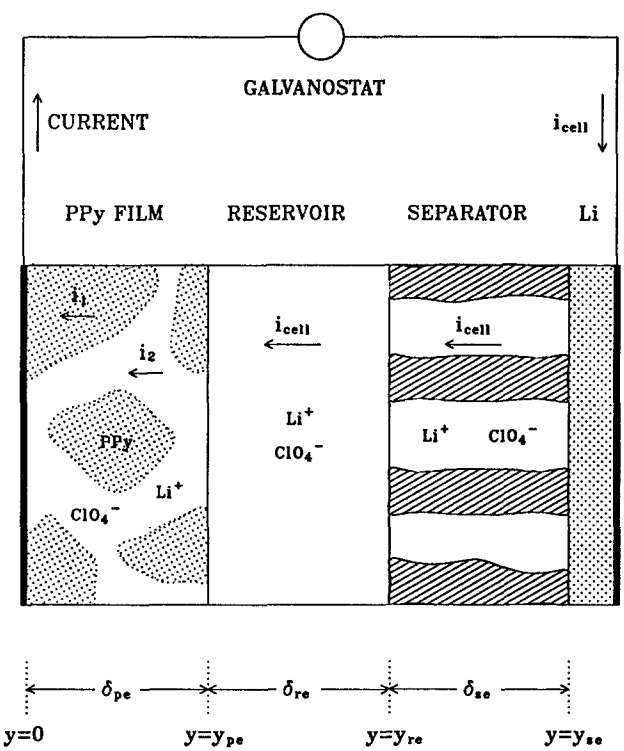

Fig. 1. Schematic of a typical $Li/LiClO_4$-PC/PPy secondary battery cell

*Electrochemical Society Student Member.
**Electrochemical Society Active Member.

coated with PPy film as a positive electrode, an electrolyte reservoir, a separator, and a lithium negative electrode. The electrolyte in this case consists of 1*M* $LiClO_4$ in propylene carbonate and is referred to as a binary electrolyte because it is assumed that $LiClO_4$ dissociates in propylene carbonate into charged Li^+ and ClO_4^- species (9). Before the descriptive equations for the model are presented, it is convenient to discuss the properties of materials used in this study and their mathematical treatment.

Electrochemistry.—During charge/discharge processes with a constant current density (i_{cell}), the electrochemical reaction occurring at the porous PPy positive electrode is assumed to be a doping-undoping of the perchlorate anion, *e.g.*

$$PPy^+ClO_4^- + e^- \underset{\text{charge}}{\overset{\text{discharge}}{\rightleftharpoons}} PPy^\circ + ClO_4^- \qquad [1]$$

where PPy° and PPy^+ are the reduced and oxidized forms of PPy. Here, the polymer itself loses (on charge) or gains (on discharge) electrons in its structure. The counterion (ClO_4^-) is incorporated into the solid structure of PPy to produce electrostatic neutrality and is often referred to as a dopant. The electrochemical reaction at the lithium negative electrode is assumed to be the dissolution and deposition of the lithium cation, *e.g.*

$$Li \underset{\text{charge}}{\overset{\text{discharge}}{\rightleftharpoons}} Li^+ + e^- \qquad [2]$$

Therefore, the overall reaction within the Li/PPy secondary battery cell is

$$PPy^+ClO_4^- + Li \underset{\text{charge}}{\overset{\text{discharge}}{\rightleftharpoons}} PPy^\circ + ClO_4^- + Li^+ \qquad [3]$$

Properties of electrolyte.—Measurements of the physical and structural properties of 1*M* $LiClO_4$-PC were conducted by Keller *et al.* (9, 10). The equivalent molar conductance of 1*M* $LiClO_4$-PC (Λ) was calculated by a graphical extrapolation of the equivalent conductance plotted *vs.* the square root of the concentration and was reported as 5.640 cm^2/Ω-mol. The transference number of a Li^+ (t_+) in 1*M* $LiClO_4$-PC was reported as 0.19 by the Hittorf method. From these experimental measurements, the necessary parameter values, which are currently not available from literature, can be calculated by using the relationship given by Newman (11).

The ionic equivalent conductance of species i (λ_i) in a binary electrolyte can be obtained by using the transference number of species i and the equivalent molar conductance [p. 230 of Ref. (11)]

$$\lambda_i = t_i\Lambda \qquad [4]$$

and is related to the ionic mobility of species i (u_i) by [p. 229 of Ref. (11)]

$$\lambda_i = |z_i|\mathbf{F}^2u_i \qquad [5]$$

where z_i represents the charge number of species i. The ionic diffusion coefficient for species i (D_i) can be then obtained by the Nernst-Einstein equation [p. 229 of Ref. (11)]

$$D_i = RTu_i \qquad [6]$$

The physical and transport properties of 1*M* $LiClO_4$-PC electrolyte discussed above are summarized in Table I.

Properties of PPy.—During charge and discharge processes, the PPy film normally consists of two distinct sites: the doped sites consisting of PPy^+ and undoped sites consisting of PPy° as shown in Eq. [1]. Thus, only a few measurements of the properties of the PPy film have been reported, and these are very limited, to the fully oxidized or reduced states as shown in Table II (12). One possible approach to obtain the necessary parameter values at an intermediate state is that the properties of PPy at an intermediate state can be considered as functions of its doping (oxidation) state (13).

Table I. Physical and transport properties of 1*M* $LiClO_4$-PC electrolyte at 25°C

Equivalent molar conductance (Λ)	5.640 cm^2/Ω-mol[a]
Transference number for Li^+ ion (t_+)	0.190[a]
Transference number for ClO_4^- ion (t_-)	0.810[a]
Ionic conductance for Li^+ ion (λ_+)	1.072 cm^2/Ω-mol[b]
Ionic conductance for ClO_4^- ion (λ_-)	4.568 cm^2/Ω-mol[b]
Mobility for Li^+ ion (u_+)	1.151×10^{-10} cm^2-mol/J-s[b]
Mobility for ClO_4^- ion (u_-)	4.907×10^{-10} cm^2-mol/J-s[b]
Diffusion coefficient for Li^+ ion (D_+)	2.853×10^{-7} cm^2/s[b]
Diffusion coefficient for ClO_4^- ion (D_-)	1.216×10^{-6} cm^2/s[b]
Reference concentration of Li^+ ion ($c_{+,ref}$)	0.001 mol/cm^3[b]
Reference concentration of ClO_4^- ion ($c_{-,ref}$)	0.001 mol/cm^3[b]

[a] Obtained from Ref. (10).
[b] Calculated by using relationship given in Ref. (11).

It is convenient to define the fraction factor of the doping level of PPy, θ, as follows

$$\theta = \frac{\lambda}{\lambda_{max}} \qquad [7]$$

where λ represents the degree of the partial oxidation of PPy (*i.e.*, the ratio of one doped anion to the number of pyrrole monomer units) and λ_{max} represents the maximal doping level. Since θ varies linearly with the amount of oxidized PPy, θ can be expressed by the consumed faradaic charge of the PPy film, Q_f, as follows

$$\theta = \frac{Q_f - Q_{f,red}}{Q_{f,oxd} - Q_{f,red}} \qquad [8]$$

where the subscripts, oxd and red, represent the fully oxidized and reduced states. It is noted that $\theta = 0$ for a fully reduced PPy film with a minimal faradaic charge, $Q_{f,red}$, and $\theta = 1$ for a fully oxidized PPy film with a maximal faradaic charge, $Q_{f,oxd}$.

The microscopic structures and the properties of the PPy electrode at intermediate state can be considered as functions of $\theta = 0$ as summarized in Table III. The porosity of the PPy film, ϵ_p, is governed by a material balance on the solid phase because the density of the PPy changes with doping level due to the amount of doped anion, and can be expressed in terms of θ as follows (14)

$$\epsilon_p = \theta\epsilon_{oxd} + (1 - \theta)\epsilon_{red} \qquad [9]$$

where θ represents the amount of oxidized PPy and $(1 - \theta)$ represents the amount of reduced PPy. The electronic conductivity of PPy film (σ_p) is obtained in a like manner (14)

$$\sigma_p = \theta\sigma_{oxd} + (1 - \theta)\sigma_{red} \qquad [10]$$

Model Development

The model presented here is for predicting the charge/discharge behavior of the Li/PPy secondary battery cell at a constant current density (i_{cell}). Figure 1 shows that the model of the cell consists of three main regions, two boundaries, and two interfaces. One of the boundaries is on the left at $y = 0$, and is used to represent the interface between a platinum current collector and the PPy positive electrode. The first region (region 1) on the left is a porous PPy positive electrode of width δ_{pe}. The first interface is between the PPy positive electrode and a reservoir at $y = y_{pe}$. The second region (region 2) is an electrolyte reservoir of width δ_{re}. The second interface is between the reser-

Table II. Properties of PPy film

Maximal doping level of PPy film (λ_{max})	0.30[a]
Faradaic charge of fully oxidized PPy film ($Q_{f,oxd}$)	120.0 C/cm^3
Faradaic charge of fully reduced PPy film ($Q_{f,red}$)	1.0×10^{-5} C/cm^3
Porosity of fully oxidized PPy film (ϵ_{oxd})	7.0×10^{-3}
Porosity of fully reduced PPy film (ϵ_{red})	1.0×10^{-2}
Conductivity of fully oxidized PPy film (σ_{oxd})	200.0/Ω-cm[b]
Conductivity of fully reduced PPy film (σ_{red})	1.0×10^{-5}/Ω-cm[b]

[a] Obtained from Ref. (5).
[b] Obtained from Ref. (12).

Table III. Summary of electrochemical properties of PPy film as functions of its doping state

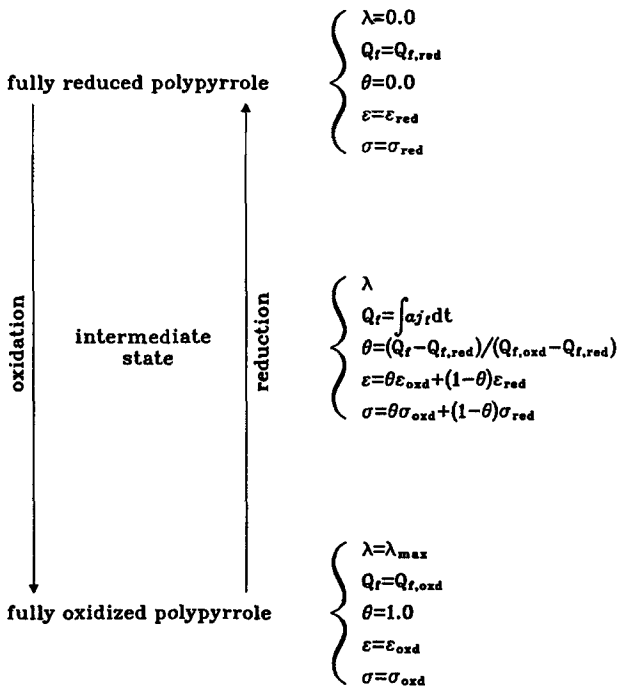

voir and a separator at $y = y_{re}$. The third region (region 3) is the separator of width δ_{se}. The second boundary condition is at $y = y_{se}$ and is between the separator and the lithium negative electrode.

In all of the regions of the cell, the unknowns are the concentration of Li^+ (c_+), the concentration of ClO^- (c_-), the local faradaic charge per unit volume (Q_f), the potential of the solid phase (Φ_1), and the potential of the solution phase (Φ_2). Values for the unknowns depend on the perpendicular distance from the platinum current collector of the PPy positive electrode (y) and time (t), and they are obtained by solving the system of governing equations and assumptions for each region of the cell described next.

Porous polypyrrole positive electrode.—Since the PPy positive electrode region consists of a solid phase of conducting polymer and a solution phase of an organic electrolyte that penetrates the void spaces in the porous structure, Newman's (15) porous electrode theory is applied to this region. Macroscopic properties are used to describe physically the porous material in terms of simple measurable parameters without regard to the actual geometrical details of the pore structure. Two of these properties are the porosity (ϵ_p) and the tortuosity (τ). The porosity represents the void volume fraction occupied by the electrolyte within a volume element of the electrode. The tortuosity is a property of the porous structure and is assumed to be related simply to the porosity as follows (16)

$$\tau = \epsilon_p^{-ex} \quad [11]$$

where ex is a constant and is set equal to 0.5 here.

The properties of the electrolyte within the PPy positive electrode (diffusivity, mobility, ionic conductivity, etc.) must be modified to account for the porous nature of this region. The effective diffusivity ($D_{i,p}$) and mobility ($u_{i,p}$) of species i within the porous structure are related to the free stream diffusivity (D_i) and mobility (u_i) as follows (16)

$$D_{i,p} = D_i\epsilon_p^{1+ex} \quad [12]$$

$$u_{i,p} = u_i\epsilon_p^{1+ex} \quad [13]$$

The effective solution conductivity (κ_p) within the porous structure, which is related to the solution concentration and free stream solution conductivity (κ), can be expressed as follows

$$\kappa_p = \kappa\epsilon_p^{1+ex} \quad [14]$$

where

$$\kappa = F^2 \sum_i z_i^2 u_i c_i \quad [15]$$

Material balance for dissolved species.—To account for the non-homogeneous structure of the PPy film, averaging is applied to the local variables within a volume element throughout the porous PPy positive electrode (15). The differential material balance equation is formulated for a dissolved species i in terms of average quantities as follows (15)

$$\frac{\partial \epsilon_p c_i}{\partial t} = -\nabla \cdot N_{i,p} + R'_{1,i} \quad [16]$$

where c_i represents the concentration of species i per unit volume of electrolyte within the porous matrix, $\epsilon_p c_i$ represents the average concentration per total unit volume including the solid polymer phase and the electrolyte that occupies the space within the matrix, and $R'_{1,i}$ is the consumption or production rate of species i due to a pseudo-homogeneous reaction (electrochemical reaction [1]) or double layer charging within the porous PPy electrode.

The flux of species i within the porous region ($N_{i,p}$) is due to migration in the electric field and diffusion in the concentration gradient and is expressed as follows (15)

$$N_{i,p} = -z_i u_{i,p} F c_i \nabla\Phi_2 - D_{i,p}\nabla c_i \quad [17]$$

where Φ_2 is the potential in the solution phase within the porous region.

The consumption or production rate of species i within the porous PPy electrode ($R'_{1,i}$) is due to a pseudo-homogeneous reaction (electrochemical reaction [1]) and double layer charging (11)

$$R'_{1,i} = -\frac{s_{1,i}}{n_1 F} a j_1 \quad [18]$$

where $s_{1,i}$ is the stoichiometric coefficient of species i for the electrochemical reaction [1], n_1 is the number of electrons transferred for the electrochemical reaction [1], a is the specific interfacial area per unit volume, and j_1 is the transfer current density (*i.e.*, current passed per unit of electroactive surface area, A/cm^2), as discussed below in the Transfer current section. It should be noted that $s_{1,i}$ is positive for an anodic reactant and negative for a cathodic reactant.

A one-dimensional material balance equation for species i can be obtained by substituting Eq. [17] and [18] into Eq. [16]

$$\frac{\partial \epsilon_p c_i}{\partial t} = z_i F\left(\frac{\partial u_{i,p}}{\partial y} c_i \frac{\partial \Phi_2}{\partial y} + u_{i,p}\frac{\partial c_i}{\partial y}\frac{\partial \Phi_2}{\partial y} + u_{i,p} c_i \frac{\partial^2 \Phi_2}{\partial y^2}\right) + \left(\frac{\partial D_{i,p}}{\partial y}\frac{\partial c_i}{\partial y} + D_{i,p}\frac{\partial^2 c_i}{\partial y^2}\right) - \frac{s_{1,i}}{n_1 F} a j_i \quad [19]$$

Current density.—The total current density flowing through the cell (i_{cell}), as shown in Fig. 1, is defined to be the sum of the superficial current density in the solid phase (i_1) and the superficial current density in the solution phase (i_2)

$$i_{cell} = i_1 + i_2 \quad [20]$$

It is assumed that the superficial current density in the solid phase (i_1) is due to the movement of electrons and is governed by Ohm's law (15)

$$i_1 = -\sigma_p \frac{\partial \Phi_1}{\partial y} \quad [21]$$

and the superficial current density in the solution phase (i_2) is due to the movement of charged species (11)

$$i_2 = F \sum_i z_i N_{i,p} \quad [22]$$

Substituting the y component of Eq. [17] into Eq. [22] yields

$$i_2 = -\kappa_p \frac{\partial \Phi_2}{\partial y} - \mathbf{F} \sum_i z_i D_{i,p} \frac{\partial c_i}{\partial y} \quad [23]$$

where κ_p is the effective conductivity of the solution phase defined in Eq. [14]. The second term on the right in Eq. [23] represents the concentration potential; this term will disappear if the ionic diffusion coefficients are all the same, which is not the case here. Substituting Eq. [21] and [23] into Eq. [20] yields

$$i_{cell} = -\sigma_p \frac{\partial \Phi_1}{\partial y} - \kappa_p \frac{\partial \Phi_2}{\partial y} - \mathbf{F} \sum_i z_i D_{i,p} \frac{\partial c_i}{\partial y} \quad [24]$$

Transfer current.—The local transfer current per unit volume, aj_1, is defined by the current transferred from the solution phase to the solid phase as follows

$$aj_1 = -\nabla \cdot i_1 = \nabla \cdot i_2 \quad [25]$$

Substituting Eq. [23] into Eq. [25] yields

$$aj_1 = -\kappa_p \frac{\partial^2 \Phi_2}{\partial y^2} - \frac{\partial \kappa_p}{\partial y} \frac{\partial \Phi_2}{\partial y} - \mathbf{F} \sum_i z_i D_{i,p} \frac{\partial^2 c_i}{\partial y^2} - \mathbf{F} \sum_i z_i \frac{\partial D_{i,p}}{\partial y} \frac{\partial c_i}{\partial y} \quad [26]$$

The local transfer current consists of two terms (17-18)

$$aj_1 = aj_f + aj_c \quad [27]$$

where aj_f and aj_c represent the faradaic and capacitive transfer current per unit volume, respectively.

The faradaic transfer current per unit volume can be expressed in terms of the rate of electrochemical reaction [1], which is controlled primarily by the available electroactive surface area and the transport rate (diffusion and migration) of the counterion, and is assumed to be given by the Butler-Volmer equation as follows (8)

$$aj_f = ai_{o1,ref} \left\{ (1-\theta) \left(\frac{c_-}{c_{-,ref}} \right) \exp\left(\frac{\alpha_{a1} \mathbf{F}}{RT} \eta_1 \right) - \theta \exp\left(\frac{-\alpha_{c1} \mathbf{F}}{RT} \eta_1 \right) \right\} \quad [28]$$

where a is the specific interfacial area per unit volume, $i_{o1,ref}$ is the exchange current density for the reaction [1] at a given reference concentration ($c_{i,ref}$), α_{a1} and α_{c1} are anodic and cathodic transfer coefficients, and η_1 is the overpotential for the reaction [1]. The term, $\alpha(1-\theta)$, represents the available electroactive surface area for anodic reaction (oxidation) and $a\theta$ represents the available electroactive surface area for cathodic reaction (reduction). Note that the fractional doping level θ, which depends on Q_f (see Eq. [8]), is assumed to be a multiplicative factor in the cathodic portion of the Butler-Volmer equation. Thus, before charging of the PPy film (*i.e.*, with $\theta = 0$), no charge can be extracted from the film. Anodic and cathodic current densities are taken to be positive and negative, respectively. Note also that $\alpha_{a1} + \alpha_{c1} = n_1$.

The overpotential is defined as

$$\eta_1 = (\Phi_1 - \Phi_{re}) - (\Phi_2 - \Phi_{re}) - U_1 \quad [29]$$

where Φ_{re} is a reference potential and U_1 is the theoretical open-circuit potential for reaction [1] at a given concentration (c_i). U_1 is given by

$$U_1 = U_{1,ref} - \frac{RT}{n_1 \mathbf{F}} \ln\left(\frac{\theta}{1-\theta} \right) \quad [30]$$

where $U_{1,ref}$ is the open-circuit potential for reaction [1] at a given reference concentration ($c_{i,ref}$). It can be seen that the local transfer current predicted by the Butler-Volmer kinetic expression, Eq. [28], depends on the difference between the potential of the solid phase and that of the adjacent solution within the porous electrode.

The rate of accumulation of the faradaic charge within the PPy film per unit volume, Q_f, is assumed to be related to the faradaic transfer current, aj_f, as follows

$$\frac{\partial Q_f}{\partial t} = aj_f \quad [31]$$

Substituting Eq. [28] into Eq. [31] yields faradaic charge balance for PPy film

$$\frac{\partial Q_f}{\partial t} = ai_{o1,ref} \left\{ (1-\theta) \left(\frac{c_-}{c_{-,ref}} \right) \exp\left(\frac{\alpha_{a1} \mathbf{F}}{RT} \eta_1 \right) - \theta \exp\left(\frac{-\alpha_{c1} \mathbf{F}}{RT} \eta_1 \right) \right\} \quad [32]$$

The anodic faradaic current transferred across the porous PPy film causes reaction [1] to proceed in the anodic direction and causes charging of the double layer within the pores of the PPy film in a manner consistent with that proposed by Feldberg (19). That is, the amount of capacitive charge that goes to charging the double layers within the pores of the porous film, Q_c, is related to the amount of the faradaic charge added to the polymer film by the faradaic reaction, Q_f. Thus, capacitive charge within the PPy film per unit volume, Q_c, can be written by

$$Q_c = a^* (\eta - \eta_{pzc}) Q_f \quad [33]$$

where a^* is a proportional constant which is assumed to be independent of potential and η_{pzc} is the total overpotential across the double layer at the point of zero charge (pzc) which is given by

$$\eta_{pzc} = \{(\Phi_1 - \Phi_{re}) - (\Phi_2 - \Phi_{re}) - U_1\}_{pzc} \quad [34]$$

Differentiating Eq. [33] yields capacitive charge balance for PPy film

$$\frac{\partial Q_c}{\partial t} = a^* \left(Q_f \frac{\partial \eta}{\partial t} + (\eta - \eta_{pzc}) \frac{\partial Q_f}{\partial t} \right) \quad [35]$$

with the assumption that $\Phi_{re} = (\Phi_{re})_{pzc}$. Because the rate of accumulation of the capacitive charge is related to the capacitive transfer current, aj_c

$$aj_c = a^* \left(Q_f \frac{\partial \eta}{\partial t} + (\eta - \eta_{pzc}) \frac{\partial Q_f}{\partial t} \right) \quad [36]$$

The total charge accumulated within the PPy film per unit volume (Q_t) is defined to be the sum of the faradaic charge (Q_f) and capacitive charge (Q_c)

$$Q_t = Q_f + Q_c \quad [37]$$

The parameter values used to simulate the electrochemical reaction rate and the double layer charge in the PPy positive electrode have been summarized in Table IV.

Reservoir.—The reservoir is the region between the PPy positive electrode and the separator, and is filled with the

Table IV. Kinetic parameter values of polypyrrole positive electrode

$ai_{o1,ref}$	10.0 A/cm^3
$U_{1,ref}$	3.087V (*vs.* Li)
n_1	1
α_{a1}	0.7
α_{c1}	0.3
$s_{1,1}$	0
$s_{1,2}$	1
a^*	2.8/V[a]
η_{pzc}	2.7V (*vs.* Li)[a]

[a] Obtained from Ref. (14).

electrolyte, 1*M* $LiClO_4$-PC (see Fig. 1). The flux of species i within the reservoir (N_i) is

$$N_i = -z_i u_i \mathbf{F} c_i \nabla \Phi_2 - D_i \nabla c_i \quad [38]$$

Substituting Eq. [38] into Eq. [16], with R'_i equal to zero and ϵ_p equal to one, yields the material balance for a dissolved species i within the reservoir

$$\frac{\partial c_i}{\partial t} = z_i u_i \mathbf{F} \left(c_i \frac{\partial^2 \Phi_2}{\partial y^2} + \frac{\partial c_i}{\partial y} \frac{\partial \Phi_2}{\partial y} \right) + D_i \left(\frac{\partial^2 c_i}{\partial y^2} \right) \quad [39]$$

Since all the current flowing through the reservoir is carried by the electrolyte, the total current density (i_{cell}) is expressed by the superficial current density in the solution phase (i_2) which is similar to that used in the positive electrode region except that the free stream conductivity (κ) and diffusivity (D_i) apply (see Eq. [23])

$$i_2 = -\kappa \frac{\partial \Phi_2}{\partial y} - \mathbf{F} \sum_i z_i D_i \frac{\partial c_i}{\partial y} = i_{cell} \quad [40]$$

Since there is no solid material, the faradaic charge (Q_f) and the solid potential (Φ_1) are treated as dummy variables and are arbitrarily set equal to zero

$$Q_f = 0 \quad [41]$$

$$\Phi_1 = 0 \quad [42]$$

Separator.—The separator consists of a porous inert material which is mainly used to prevent physical contact between the PPy positive electrode and the Li negative electrode, and a solution phase which fills the void spaces of the porous structure. Since the solid material is inert, the porosity does not change with time and is set arbitrarily equal to a constant (*i.e.*, $\epsilon_s = 0.5$). An effective diffusivity ($D_{i,s}$) and mobility ($u_{i,s}$) of species i and ionic conductivity of electrolyte (κ_s) within the separator are obtained in the same manner as that for the PPy positive electrode region (see Eq. [12]-[14])

$$D_{i,s} = D_i \epsilon_s^{1+ex} \quad [43]$$

$$u_{i,s} = u_i \epsilon_s^{1+ex} \quad [44]$$

$$\kappa_s = \kappa \epsilon_s^{1+ex} \quad [45]$$

The flux of species i within the separator ($N_{i,s}$) is also given by an equation that is similar to that for the PPy positive electrode (see Eq. [17])

$$N_{i,s} = -z_i u_{i,s} \mathbf{F} c_i \nabla \Phi_2 - D_{i,s} \nabla c_i \quad [46]$$

In this case, mass transfer in the separator is governed by a differential material balance equation for species i

$$\epsilon_s \frac{\partial c_i}{\partial t} = z_i u_{i,s} \mathbf{F} \left(c_i \frac{\partial^2 \Phi_2}{\partial y^2} + \frac{\partial c_i}{\partial y} \frac{\partial \Phi_2}{\partial y} \right) + D_{i,s} \left(\frac{\partial^2 c_i}{\partial y^2} \right) \quad [47]$$

Since the solid material is inert and all the current flowing through the separator is carried by the electrolyte, the total current density (i_{cell}) in this region is expressed by the superficial current density in the solution phase (i_2), which is similar to that used in the reservoir, with the exception that the effective conductivity (κ_s) and diffusivity ($D_{i,s}$) apply (see Eq. [40])

$$i_2 = -\kappa_s \frac{\partial \Phi_2}{\partial y} - \mathbf{F} \sum_i z_i D_{i,s} \frac{\partial c_i}{\partial y} = i_{cell} \quad [48]$$

Boundary and interface conditions.—To complete the system of equations for the model, the boundary conditions at each end of the cell and inter-regional interfaces must be specified for the dependent variables: c_+, c_-, Q_f, Φ_1, and Φ_2. Boundary and interface conditions for these dependent variables are specified in the order of the positive electrode to the negative electrode. The porous PPy positive electrode is bounded by a platinum current collector on one face ($y = 0$) and by the reservoir on the other ($y = y_{pe}$). At the current collector/PPy positive electrode interface ($y = 0$), the normal component of the flux of Li^+ is assumed to be equal to zero

$$-z_+ u_{+,p} \mathbf{F} c_+ \frac{\partial \Phi_2}{\partial y} - D_{+,p} \frac{\partial c_+}{\partial y} = 0 \quad [49]$$

The rate of consumption (charge) or production (discharge) of ClO_4^- by the electrochemical reaction [1] is equal to the net normal component of the flux of ClO_4^- towards or away from the electrode

$$-z_- u_{-,p} \mathbf{F} c_- \frac{\partial \Phi_2}{\partial y} - D_{-,p} \frac{\partial c_-}{\partial y} = \frac{a s_{1,-}}{n_1 \mathbf{F}} j_1 \quad [50]$$

The rate of accumulation of the faradaic charge within the PPy film per unit volume, Q_f, is obtained by Eq. [32]. At this point, all the current leaves the cell via the current collector, which can be represented with constant i_{cell}

$$i_1 = -\sigma_p \frac{\partial \Phi_1}{\partial y} = i_{cell} \quad [51]$$

$$i_2 = -\kappa_p \frac{\partial \Phi_2}{\partial y} - \mathbf{F} \sum_i z_i D_{i,p} \frac{\partial c_i}{\partial y} = 0 \quad [52]$$

At the PPy positive electrode/reservoir interface, the flux of each species i across the two regions must be continuous, which can be written as follows

$$-z_i u_{i,p} \mathbf{F} c_i \frac{\partial \Phi_2}{\partial y} - D_{i,p} \frac{\partial c_i}{\partial y} = -z_i u_i \mathbf{F} c_i \frac{\partial \Phi_2}{\partial y} - D_i \frac{\partial c_i}{\partial y} \quad [53]$$

In a similar manner, the superficial current density (i_2) in the solution phase is also taken to be continuous across this interface, so that

$$i_2 = -\kappa_p \frac{\partial \Phi_2}{\partial y} - \mathbf{F} \sum_i z_i D_{i,p} \frac{\partial c_i}{\partial y} = i_{cell} \quad [54]$$

Because the solid electrode phase ends at this point and all of the current is in the solution phase, the gradient of the faradaic charge and the solid potential are set equal to zero

$$\left. \frac{\partial Q_f}{\partial y} \right|_{y_{pe}} = 0 \quad [55]$$

$$\left. \frac{\partial \Phi_1}{\partial y} \right|_{y_{pe}} = 0 \quad [56]$$

At the reservoir/separator interface, the boundary conditions are derived in the same manner as those for the positive electrode/reservoir interface. The flux of each species i and the superficial current density in the solution phase across the two regions must be continuous

$$-z_i u_i \mathbf{F} c_i \frac{\partial \Phi_2}{\partial y} - D_i \frac{\partial c_i}{\partial y} = -z_i u_{i,s} \mathbf{F} c_i \frac{\partial \Phi_2}{\partial y} - D_{i,s} \frac{\partial c_i}{\partial y} \quad [57]$$

$$i_2 = -\kappa_s \frac{\partial \Phi_2}{\partial y} - \mathbf{F} \sum_i z_i D_{i,s} \frac{\partial c_i}{\partial y} = i_{cell} \quad [58]$$

At this interface, Q_f and Φ_1 are treated as dummy variables and are arbitrarily set equal to zero.

At the separator/Li negative electrode interface, the rate of consumption (charge) or production (discharge) of a Li^+ by the electrochemical reaction [2] is equal to the net normal component of the flux of Li^+ towards or away from the electrode (20)

$$-z_+ u_{+,s} \mathbf{F} c_+ \frac{\partial \Phi_2}{\partial y} - D_{+,s} \frac{\partial c_+}{\partial y} = \frac{s_{2,+}}{n_2 \mathbf{F}} j_2 \quad [59]$$

The normal component of the flux of ClO_4^- is assumed to be equal to zero at $y = y_{se}$

$$-z_{-}u_{-,s}\mathbf{F}c_{-}\frac{\partial\Phi_2}{\partial y} - D_{-,s}\frac{\partial c_{-}}{\partial y} = 0 \qquad [60]$$

The potential in the solid lithium (Φ_1) at this point is set arbitrarily equal to zero volts

$$\Phi_1 = 0 \qquad [61]$$

This is done to provide a reference point and consequently a particular solution for the model. Of course, Φ_1 could be alternatively set to zero at the other end of the cell (*i.e.*, at the current collector/PPy positive electrode interface). At this point ($y = y_{se}$), all the current in the cell leaves the electrolyte and enters the lithium negative electrode by the electrochemical reaction [2]

$$j_2 = -i_{cell} \qquad [62]$$

The electrochemical reaction of the Li negative electrode during charge/discharge is given by Eq. [2]. The rate of this reaction is controlled primarily by the transport rate (diffusion and migration) of the lithium cation and can be expressed by the faradaic transfer current density for reaction [2], j_2, which is assumed to be given by the Butler-Volmer equation as follows (14)

$$j_2 = i_{o2,ref}\left\{\exp\left(\frac{\alpha_{a2}\mathbf{F}}{RT}\eta_2\right) - \exp\left(\frac{-\alpha_{c2}\mathbf{F}}{RT}\eta_2\right)\right\} \qquad [63]$$

where $i_{0,2,ref}$ represents the exchange current density for reaction [2] at a given reference concentration ($c_{i,ref}$), α_{a2} and α_{c2} represent the transfer coefficients for the anodic and the cathodic direction of the electrochemical reaction [2], and η_2 is the overpotential for reaction [2]. Again, $\alpha_{a2} + \alpha_{c2} = n_2$.

The overpotential is defined as

$$\eta_2 = (\Phi_1 - \Phi_{re}) - (\Phi_2 - \Phi_{re}) - U_2 \qquad [64]$$

where U_2 is the theoretical open-circuit potential for reaction [2] at the given concentration (c_i) and is given by

$$U_2 = U_{2,ref} - \frac{RT}{n_2\mathbf{F}}\ln\left(\frac{c_i}{c_{i,ref}}\right) \qquad [65]$$

Here, $U_{2,ref}$ is the open-circuit potential for reaction [2] at a given reference concentration ($c_{i,ref}$).

Substituting Eq. [63] into Eq. [62] yields

$$i_{o2,ref}\left\{\exp\left(\frac{\alpha_{a2}\mathbf{F}}{RT}\eta_2\right) - \exp\left(\frac{-\alpha_{c2}\mathbf{F}}{RT}\eta_2\right)\right\} = -i_{cell} \qquad [66]$$

The parameter values used to simulate the electrochemical reaction rate of the lithium negative electrode are summarized in Table V. According to Jasinski (9), it can be concluded that Li/Li^+ has a high exchange current density in 1*M* $LiClO_4$-PC; at least on the order of 2-5 mA/cm^2 for a smooth surface and a cathodic transfer coefficient (α_{c2}) ranged from 0.66 to 0.72.

Initial conditions.—Initial conditions are necessary for the variables which depend explicitly on time. For convenience, it is assumed that the cell is fully discharged and ready to be charged. Consequently, the faradaic charge per unit volume in the PPy film (Q_f) is initially set equal to $Q_{f,red}$, a minimal charge state. Therefore, porosity (ϵ_p) and conductivity (σ_p) of the PPy film are initially set equal to ϵ_{red} and σ_{red}, values at this reduced state. The concentration of each species i throughout the cell is set equal to its reference concentration

$$c_i = c_{i,ref} \qquad [67]$$

The conductivity of the electrolyte (κ) can be obtained by combining Eq. [15] and [67]. The other dependent variables (Φ_1 and Φ_2) do not require initial conditions and were arbitrarily set equal to zero at $t = 0$ for all y.

Solution method.—The governing equations, boundary conditions, and interface conditions for the determination of the quantities c_+, c_-, Q_f, Φ_1, and Φ_2 have been summarized in Table VI. The system of equations was put into finite difference form and solved as a function of time and position by using a numerical technique referred to as Newman's pentadiagonal block matrix equation solver (21) and implicit stepping (22). Once the values of unknowns (c_+, c_-, Q_f, Φ_1, and Φ_2) are obtained, values of i_1 and i_2 for each region, and Q_c, can be obtained from those dependent variables using Eq. [21], [23], and [33]. The total current density (i_{cell}) flowing through the cell is constant and is equal to the sum of the current density flowing in the solid phase (i_1) and the solution phase (i_2).

Results and Discussion

The model can be used to simulate the charge and discharge dynamic behavior of a typical $Li/LiClO_4$-PC/PPy secondary battery cell under various operating conditions. The effects of various design parameters, such as the thickness of the electrode, the reservoir, and the separator, etc., on the cell discharge performance could also be examined, if desired.

The fixed parameter values in predicting the performance of the Li/PPy cell are given in Table VII. A one μm thick PPy film was used in this paper because a high doping level and a high efficiency have been observed for this thickness (5). To minimize ohmic loss in a cell, the separator was chosen to have an overall porosity of 0.5 to permit better diffusion and migration of the ions between the electrodes. The thickness of the reservoir and the separator were chosen arbitrarily to contain 30% electrolyte for a fully charged cell. Separators as thick as 25 μm would

Table V. Kinetic parameter values of lithium negative electrode

$i_{o2,ref}$	0.002 A/cm^2 [a]
$U_{2,ref}$	0.0V (*vs.* Li)
n_2	1
α_{a2}	0.3[a]
α_{c2}	0.7[a]
$s_{2,1}$	−1
$s_{2,2}$	0

[a] Obtained from Ref. (9).

Table VI. System of equations[a]

A. Governing equations

Variables	Region 1	Region 2	Region 3
c_+	19	39	47
c_-	19	39	47
Q_f	32	41	41
Φ_1	26	42	42
Φ_2	24	40	48

B. Boundary and interface conditions

Variables	$y = 0$	$y = y_{pe}$	$y = y_{re}$	$y = y_{se}$
c_+	49	53	57	59
c_-	50	53	57	60
Q_f	32	55	41	41
Φ_1	51	56	42	61
Φ_2	52	54	58	66

[a] The numbers in the tables refer to the equation numbers in the text.

Table VII. Fixed parameter values

Operating temperature (T)	298.15 K
Applied cell current density (i_{cell})	0.2 mA/cm^2
Geometric electrode surface area (A)	1.0 cm^2
Thickness of PPy positive electrode (δ_{pe})	1.0 μm
Thickness of reservoir (δ_{re})	3.0 μm
Thickness of separator (δ_{se})	2.0 μm
Porosity of separator (ϵ_s)	0.5

Table VIII. Characteristic electrochemical data for a one-square-centimeter Li/PPy cell during discharge

Mass of PPy positive electrode (M)	1.51×10^{-4}g
Applied cell current (I_{cell})	0.2 mA
Average cell potential (Φ_{ave})	3.152V
Discharge time (t_d)	165.0s
Energy density	191.3 Wh/kg[a]
Power density	41.7 W/kg[a]

[a] Based on the mass of the PPy positive electrode.

cause a significant degradation in the performance of the cell. Consequently, it may be necessary to develop new methods of separator preparation to be able to build a practical cell. Parameters not referenced in Tables I through VII were selected arbitrarily.

A typical charge/discharge curve at a constant current density of 0.2 mA/cm^2 for a Li/PPy cell with 1M $LiClO_4$-PC is presented in Fig. 2. The charge and discharge current densities are specified as being positive and negative, respectively, because of the chosen coordinate system. The cell potential, Φ_{cell}, represents the difference between the potential of the solid phase at the current collector of the PPy positive electrode at $y = 0$ and that of the Li negative electrode at $y = y_{se}$. For convenience, the charge and discharge processes were terminated when the faradaic charge state of the cell ($Q_f/Q_{f,oxd}$) reached 99.9% and 0.1%, respectively.

The predicted cell potential after 99.9% charge was 3.444V. At the end of the discharge, the sharp potential drop indicates that the polymer becomes an insulator. The average discharge potential (Φ_{ave}) of a typical cell can be estimated from the discharge curve in Fig. 2 to be 3.152V. Important properties of a battery are the energy and power densities. The energy density of a cell is defined here as the amount of energy extracted per unit mass of PPy in the cell and is calculated by using the following equation (2)

$$\text{Energy density} = \frac{I_{cell}\Phi_{ave}t_d}{M} \quad [68]$$

where I_{cell} is the total cell current, t_d is the discharge time of the cell, and M is the mass of the PPy electrode. The total cell current (I_{cell}) can be obtained by multiplying by the cell current density (i_{cell}) by the cross-sectional area of the electrode (A). The theoretical energy density obtained from the discharge curve in Fig. 2 was about 191.3 Wh/kg of PPy positive electrode.

The power density of a cell is defined as the rate of delivering energy and is the product of the average cell discharge potential (Φ_{ave}) multiplied by the current of the cell (I_{cell}) as follows

$$\text{Power density} = I_{cell}\Phi_{ave} \quad [69]$$

The theoretical power density obtained from the discharge curve in Fig. 2 was about 41.7 W/kg of PPy positive electrode.

The characteristics of the cell estimated from this study are summarized in Table VIII. Direct comparison of the theoretical prediction to those of the experimental data available in the literature was not attempted, although the predictions of charge/discharge behavior seem reasonable. The kinetics of the anion doping-undoping process of a PPy electrode and the capacity of a lithium/polymer battery are strongly dependent on the morphology and the thickness of the PPy films.

The cell potential *vs.* time curve in Fig. 2 increases with a certain initial slope which changes to a different slope midway through both charge and discharge. This is because the charging and discharging processes are affected by two distinctive factors, faradaic and capacitive current densities, i_f and i_c. These are obtained by integrating the local faradaic and capacitive transfer current (aj_f and aj_c) over the porous PPy positive electrode region and are shown in Fig. 3 as a function time.

During charge, the first slope in Fig. 2 is dominated by the faradaic effect, while the second slope is dominated by

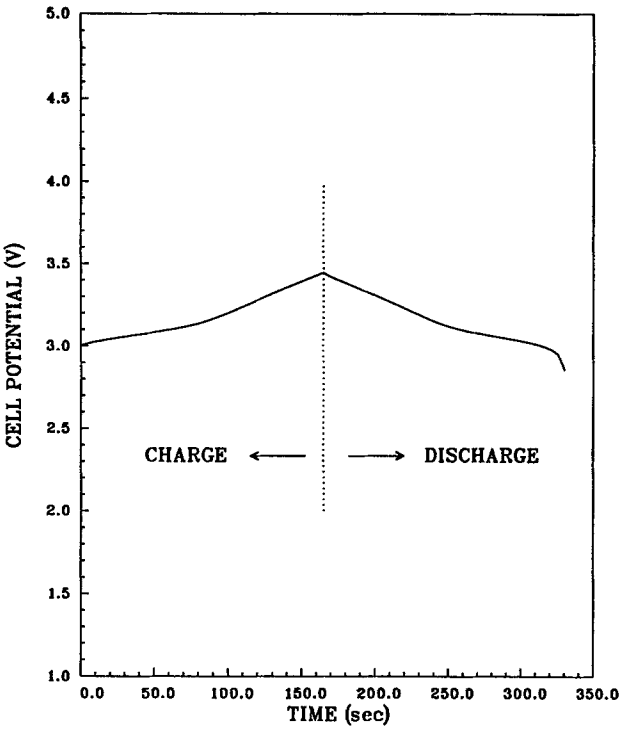

Fig. 2. Charge/discharge behavior of a typical Li/$LiClO_4$-PC/PPy secondary battery cell at i_{cell} = 0.2 mA/cm^2.

the capacitive effect. The faradaic current density (i_f) decreases with time because the electroactive area (reduced PPy sites) and the concentration of the counterion decrease as the PPy positive electrode is charged. However, the capacitive current density (i_c) increases continuously with time until the PPy electrode is fully oxidized at about 110s. When the PPy electrode is fully oxidized, the faradaic current density becomes very small (no further oxidation of the PPy film occurs) and the total current density is equal to the capacitive current density, which is used to charge the double layers within the porous PPy positive electrode.

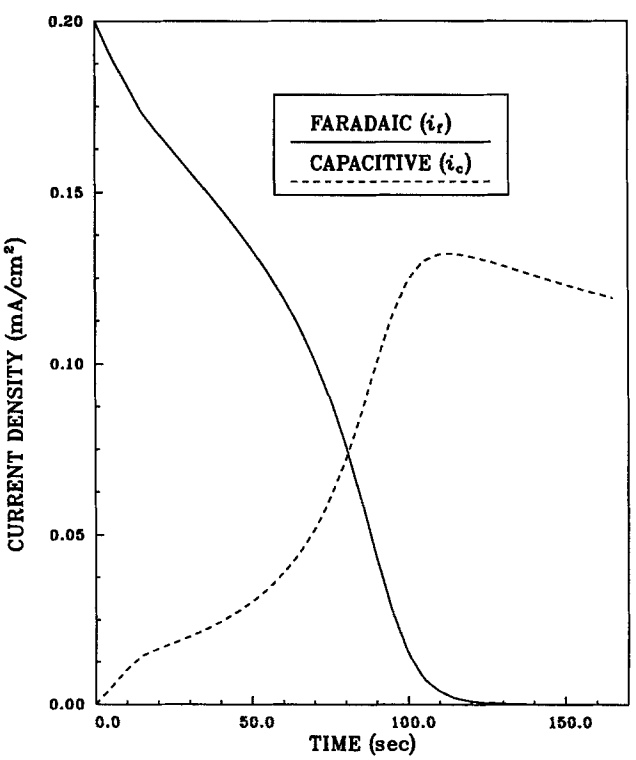

Fig. 3. Faradaic and capacitive current densities in PPy positive electrode during charge at i_{cell} = 0.2 mA/cm^2.

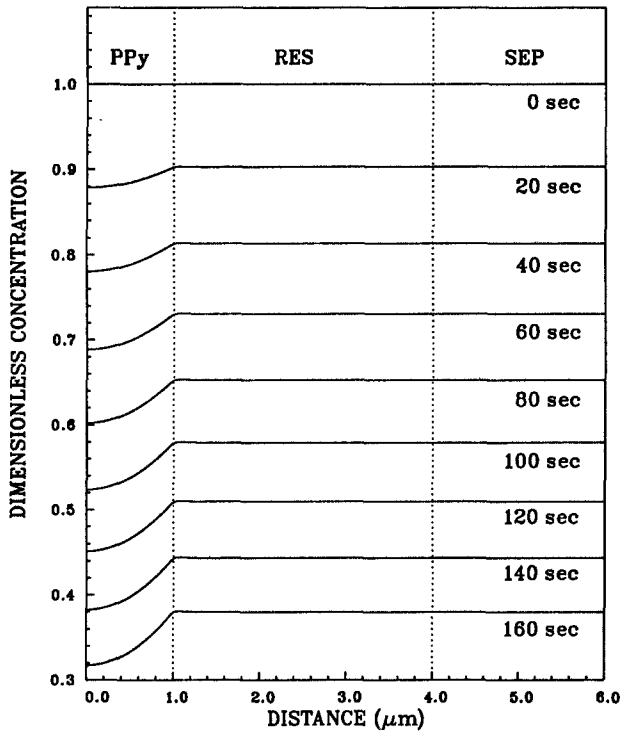

Fig. 4. Concentration profiles of the counterion (ClO_4^-) across a typical cell during charge at i_{cell} = 0.2 mA/cm^2.

Figures 4 and 5 show the profiles of the dependent variables at a constant current density of 0.2 mA/cm^2 during charge. The concentration profiles of the counterion, ClO_4^-, across a typical cell are shown in Fig. 4. For convenience, the concentration of the counterion was made dimensionless relative to its reference concentrations ($c_{-,ref}$). Initially, the concentration of the counterion is uniform throughout the cell at reference concentration ($c_{-,ref}$). Applying a constant current density of 0.2 mA/cm^2 causes the anions (ClO_4^-) to be consumed at the PPy positive electrode by the oxidation of PPy (electrochemical reaction [1]) and by double layer charging. Also, cations (Li^+) are consumed at the lithium negative electrode by the reduction of Li (electrochemical reaction [2]). The reacting species are transported from the reservoir to the electrodes where they diffuse and migrate to the reactive sites. For discharge, the opposite is true. Since the effective diffusivities of Li^+ and ClO_4^- within the porous layer are smaller than the free stream diffusivity of those species, the concentration gradients within the porous region must be larger to make up for the slower movement of the ions. The gradient within the PPy positive electrode becomes larger with time.

Figure 5 shows the distribution of faradaic charge consumed in a PPy positive electrode at a constant current density of 0.2 mA/cm^2 during charge. The faradaic charge per unit volume was made dimensionless by using the maximum faradaic charge value ($Q_{f,oxd}$) as the reference point. Initially, the PPy positive electrode is fully reduced (value of $Q_{f,red}$) and is ready to be oxidized. During charging at a constant current density of 0.2 mA/cm^2, the faradaic charge is accumulated throughout the PPy positive electrode by the electrochemical reaction [1]. The faradaic charge accumulation in the outer layer of the PPy film is faster because of the concentration gradient within PPy positive electrode as shown in Fig. 4. After the PPy positive electrode is significantly oxidized, the charge distribution becomes uniform again. During discharge, the faradaic charge is withdrawn faster in the outer layer of the PPy film for the same reason. The other electrochemical properties of the PPy positive electrode (such as porosity, electronic and ionic conductivity, diffusivity, etc.) have the same distribution throughout the PPy positive electrode because these properties are proportional to the faradaic charge consumed within the PPy positive electrode. The effects of various operating conditions can be examined. For example, the effects of discharge rate on the predicted behavior of the cell discharge are examined in Fig. 6. This clearly illustrates that the electrodes are better utilized at lower discharge rate. By discharging at a lower rate, much more energy can be drawn from the cell.

The effects of various cell physical parameters on the predicted behavior of the cell and their implications are examined in Fig. 7-9. The capacity of a Li/PPy cell is determined by the amount of electrode active material and the

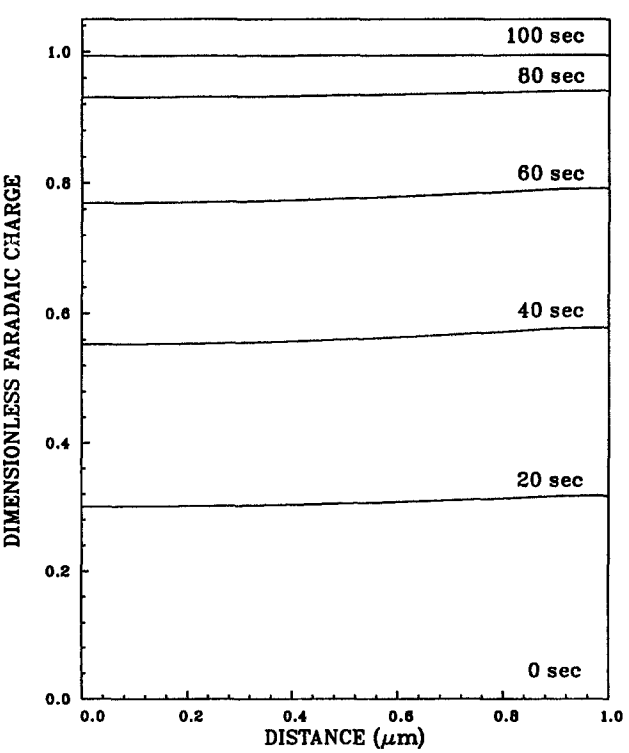

Fig. 5. Faradaic charge profiles within the PPy positive electrode during charge at i_{cell} = 0.2 mA/cm^2.

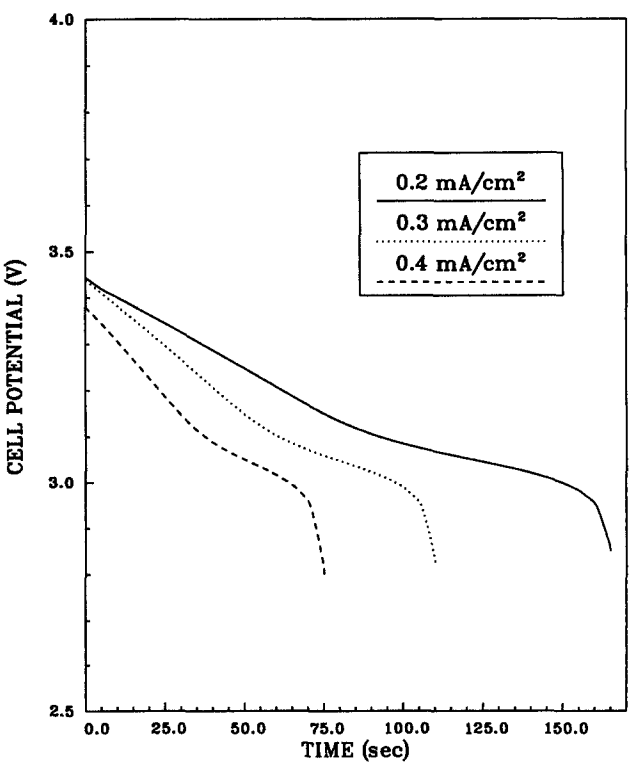

Fig. 6. The effect of the discharge rate on the cell discharge performance.

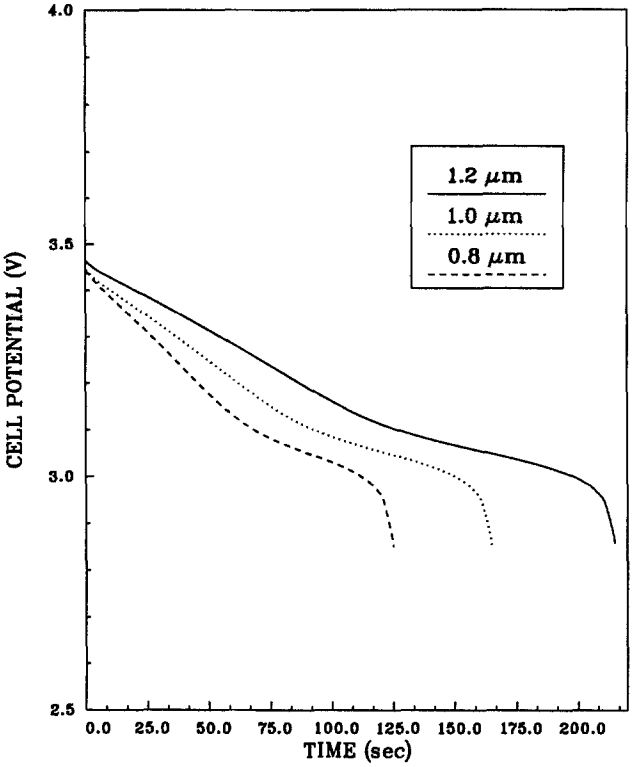

Fig. 7. The effect of the thickness of the PPy electrode on the cell discharge performance at i_{cell} = 0.2 mA/cm^2.

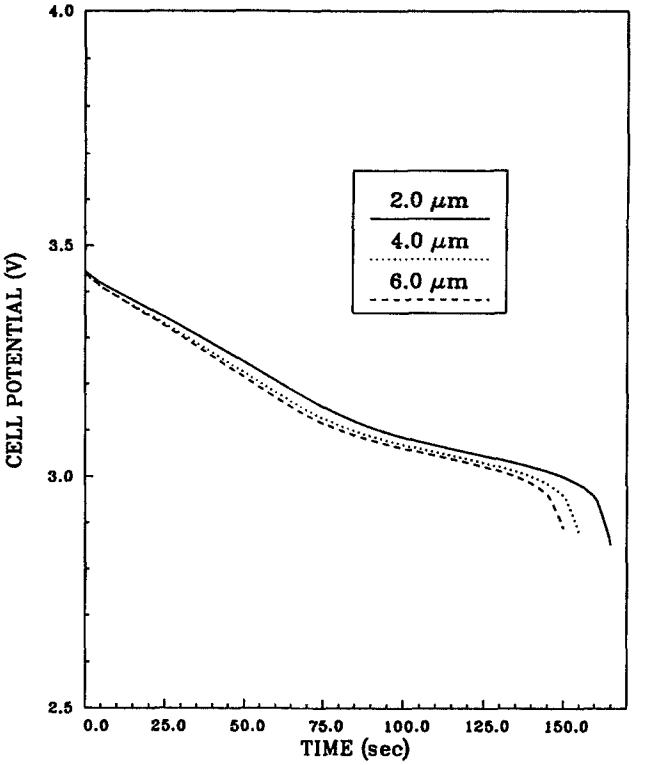

Fig. 9. The effect of the thickness of the separator on the cell discharge performance at i_{cell} = 0.2 mA/cm^2.

amount of electrolyte available in the cell. Figure 7 shows the effect of the thickness of the PPy positive electrode (equivalent to changing the amount of PPy electroactive material) on the discharge cell performance. Figure 8 shows the effect of the thickness of the reservoir (equivalent to changing the amount of electroactive counterion) on the discharge cell performance at a constant current of 0.2 mA/cm^2. Increasing the thickness of the reservoir yields a slightly smaller cell discharge potential and a shorter discharge time. This is because the thicker reservoir tends to increase ohmic drop. Figure 9 shows the effect of the thickness of the separator on the discharge cell performance at a constant current of 0.2 mA/cm^2. Also, increasing the thickness of separator yields a slightly smaller cell discharge potential and a shorter discharge time. This is because the thicker separator tends to increase ohmic drop.

Consequently, the optimal values of design parameters (such as, thickness for the PPy positive electrode, reservoir, and separator) have to be determined in conjunction with other design parameters and operating conditions.

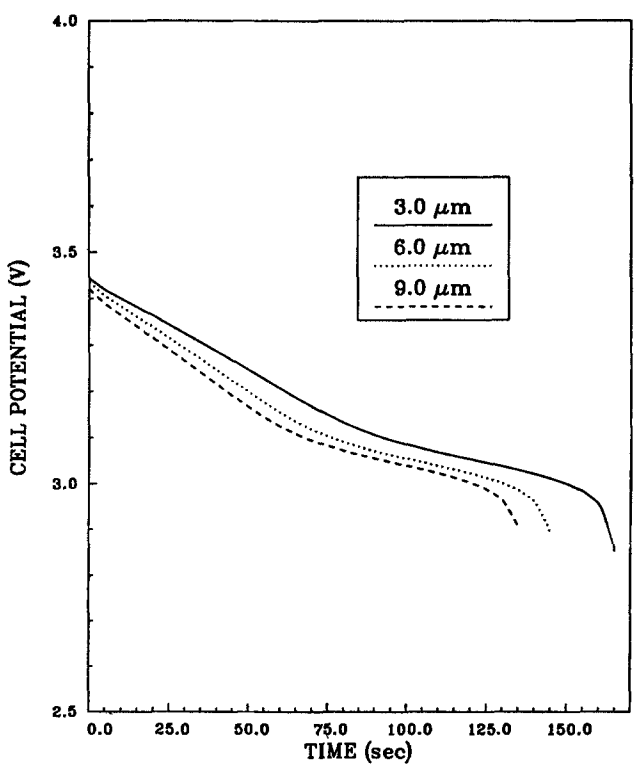

Fig. 8. The effect of the thickness of the reservoir on the cell discharge performance at i_{cell} = 0.2 mA/cm^2.

Summary

A mathematical model of a Li/PPy cell based on the dilute solution theory and the porous electrode theory was developed here to predict the dynamic behavior of a Li/$LiClO_4$-PC/PPy cell. The model includes double layer effects on the cell performance and treats the electrochemical properties of PPy as functions of its doping state. It may be possible to use this model together with experimental data and a parameter estimation technique to determine the design parameters for the best performance of the Li/$LiClO_4$-PC/PPy cell. Also, the Li/PPy model developed here could be modified to study other polymeric battery systems.

Acknowledgment

It is acknowledged gratefully that this work was supported by a National Aeronautics and Space Administration Grant (NAG-9-173).

Manuscript submitted March 6, 1989; revised manuscript received Dec. 4, 1989.

Texas A&M University assisted in meeting the publication costs of this article.

LIST OF SYMBOLS

A	geometric electrode surface area, cm^2
a	specific surface area of the porous PPy positive electrode, /cm
a^*	double layer constant, /V
c_i	concentration of species i, mol/cm^3
$c_{i,ref}$	reference concentration of species i, mol/cm^3

D_i diffusion coefficient of species i, cm^2/s
$D_{i,p}$ effective diffusion coefficient of species i in the PPy positive electrode, cm^2/s
$D_{i,s}$ effective diffusion coefficient of species i in the separator, cm^2/s
$\mathbf{F}$ Faraday's constant, 96,487 C/mol
I_{cell} applied cell current, mA
i_c capacitive current density based on projected electrode area, A/cm^2
i_{cell} applied cell current density, mA/cm^2
i_f faradaic current density based on projected electrode area, A/cm^2
$i_{oj,ref}$ exchange current density at reference concentrations for reaction j, A/cm^2
i_1 superficial current density in the solid phase, A/cm^2
i_2 superficial current density in the solution phase, A/cm^2
j_c capacitive transfer current density at the PPy positive electrode, A/cm^2
j_f faradaic transfer current density at the PPy positive electrode, A/cm^2
j_1 transfer current density at the PPy positive electrode, A/cm^2
j_2 transfer current density at the Li negative electrode, A/cm^2
M mass of the PPy positive electrode, g
N_i flux vector of species i, mol/cm^2-s
$N_{i,p}$ flux vector of species i within the PPy positive electrode, mol/cm^2-s
$N_{i,s}$ flux vector of species i within the separator, mol/cm^2-s
n_j number of electrons transferred for reaction j
Q_c capacitive charge of the PPy positive electrode per unit volume, C/cm^3
Q_f faradaic charge of the PPy positive electrode per unit volume, C/cm^3
$Q_{f,oxd}$ faradaic charge of the fully oxidized PPy film per unit volume, C/cm^3
$Q_{f,red}$ faradaic charge of the fully reduced PPy film per unit volume, C/cm^3
Q_t total charge of the PPy positive electrode per unit volume, C/cm^3
R universal gas constant, 8.3143 J/mol-K
$R'_{j,i}$ pseudohomogenous reaction rate of species i for reaction j, mol/cm^3-s
$s_{j,i}$ stoichiometric coefficient of species i for reaction j
T absolute temperature, K
t time, s
t_d discharge time of the Li/PPy cell, s
t_i transference number of species i
U_j theoretical open-circuit potential at the surface concentration for reaction j, V
$U_{j,ref}$ theoretical open-circuit potential at reference concentration for reaction j, V
u_i mobility of species i, $mol\text{-}cm^2/J\text{-}s$
$u_{i,p}$ effective mobility of species i in the PPy film, $mol\text{-}cm^2/J\text{-}s$
$u_{i,s}$ effective mobility of species i in the separator, $mol\text{-}cm^2/J\text{-}s$
y perpendicular distance from the substrate/positive electrode interface, μm
y_{pe} position of the PPy positive electrode/reservoir interface in y coordinate, μm
y_{re} position of the reservoir/separator interface in y coordinate, μm
y_{se} position of the separator/Li negative electrode interface in y coordinate, μm
z_i charge number of species i

Greek Symbols

α_{aj} anodic transfer coefficient for reaction j
α_{cj} cathodic transfer coefficient for reaction j
δ_{pe} thickness of the PPy positive electrode, μm
δ_{re} thickness of the reservoir, μm
δ_{se} thickness of the separator, μm
ϵ_{oxd} porosity of the fully oxidized PPy film
ϵ_p porosity of the PPy positive electrode
ϵ_{red} porosity of the fully reduced PPy film
ϵ_s porosity of the separator
η_j overpotential for reaction j, V
η_{pzc} overpotential at the point of zero charge, V
κ free stream solution conductivity, /Ω-cm
κ_p effective solution conductivity within the PPy film, /Ω-cm
κ_s effective solution conductivity within the separator, /Ω-cm
Λ equivalent molar conductance of binary electrolyte, cm^2/Ω-cm
λ doping level of the PPy film
λ_i ionic conductance of species i, cm^2/Ω-cm
λ_{max} maximum doping level of the PPy film, 0.30
θ fractional doping level of the PPy film
σ_{oxd} conductivity of the fully oxidized PPy film, /Ω-cm
σ_p conductivity of the PPy positive electrode, /Ω-cm
σ_{red} conductivity of the fully reduced PPy film, /Ω-cm
τ tortuosity of the PPy positive electrode
Φ_{ave} average cell discharge potential, V
Φ_{re} reference potential, V
Φ_1 potential in the solid phase, V
Φ_2 potential in the solution phase, V

Subscript

$+$ cation, Li^+
$-$ anion, ClO_4^-

REFERENCES

1. H. Münstedt, G. Köhler, H. Möhwald, D. Naegele, R. Bitthin, G. Ely, and E. Meissner, *Synth. Met.*, **18,** 259 (1987).
2. T. Osaka, K. Naoi, H. Sakai, and S. Ogano, *This Journal,* **134,** 285 (1987).
3. T. Osaka, K. Naoi, S. Ogano, and S. Nakamura, *ibid.,* **134,** 2096 (1987).
4. F. Trinidad, J. Alonso-Lopez, and M. Nebot, *J. App. Electrochem.*, **17,** 215 (1987).
5. S. Panero, P. Prosperi, and B. Scrosati, *Electrochim. Acta,* **32,** 1465 (1987).
6. K. Naoi and T. Osaka, *This Journal,* **134,** 2479 (1987).
7. K. Naoi, A. Ishijima, and T. Osaka, *J. Electroanal. Chem.*, **217,** 203 (1987).
8. T. Yeu, T. V. Nguyen, and R. E. White, *This Journal,* **135,** 1971 (1988).
9. R. Jasinski, in "Advances in Electrochemistry and Electrochemical Engineering," Vol. 8, C. W. Tobias, Editor, pp. 253-335, John Wiley & Sons, Inc., New York (1971).
10. R. Keller, J. N. Foster, D. C. Hanson, J. F. Hon, and J. S. Muirhead, "Properties of Nonaqueous Electrolyte," NAS 3-8521, NASA CR-1425 (1969).
11. J. S. Newman, "Electrochemical Systems," Prentice-Hall, Englewood Cliffs, NJ (1973).
12. M. Salmon, A. F. Diaz, A. J. Logan, M. Krounbi, and J. Bargon, *Mol. Cryst. Liq. Cryst.*, **83,** 265 (1982).
13. R. M. Penner, Ph.D. Dissertation, Texas A&M University, College Station, TX (1987).
14. T. Yeu, Ph.D. Dissertation, Texas A&M University, College Station, TX (1989).
15. J. Newman and W. Tiedemann, *AIChE J.*, **21,** 25 (1975).
16. T. V. Nguyen, Ph.D. Dissertation, Texas A&M University, College Station, TX (1990).
17. R. A. Bull, F. F. Fan, and A. J. Bard, *This Journal,* **129,** 1009 (1982).
18. P. G. Pickup and R. A. Osteryoung, *J. Electroanal. Chem.*, **195,** 271 (1985).
19. S. W. Feldberg, *J. Am. Chem. Soc.*, **106,** 4671 (1984).
20. R. E. White, S. E. Lorimer, and R. Darby, *This Journal,* **130,** 1123 (1983).
21. J. Van Zee, G. Kleine, R. E. White, and J. Newman, in "Electrochemical Cell Design," R. E. White, Editor, pp. 377-389, Plenum Press, New York (1984).
22. B. Carnahan, H. A. Luther, and J. O. Wilkes, "Applied Numerical Methods," John Wiley & Sons, New York (1969).